Testing and Radiation Qualification of the SCA Controller Engineering Prototype

D.M. Gingrich, D.A. Gish, S. Liu
University of Alberta

September 4, 2003

We describe the bench testing and radiation qualification of the SCA controller engineering prototype for the ATLAS LAr calorimeter front-end boards. From a total of 362 parts, we have determined the functional and electrical yield to be 98%. Based on the high yield and the high tolerance to radiation, we consider the SCA controller ready for production.

1 Introduction

The front-end board of the ATLAS LAr calorimeter readout uses switched capacitor array (SCA) analog memories for storage of the calorimeter signals during the level-1 trigger latency. The addressing of the SCAs and other control functions of the front-end board are managed by two SCA controller (SCAC) ASICs on each front-end board.

The front-end boards will be located on-detector, in crates mounted on the feedthroughs in the gap between the barrel and the endcap cryostats (for the EM barrel) and at the back of the endcap cryostats (for the EM endcap and hadronic endcap). The SCA controller must therefore undergo a radiation qualification procedure to ensure its suitability for use in the ATLAS environment.

The SCA controller has been implemented in a 0.25 μm CMOS process using a radiation-tolerant standard-cell library [1]. The SCA controller was submitted for prototyping on 28 February 2001 (MPW4 run). A second prototype, mainly required to add ESD protection to the I/O buffers, was submitted November 2001 (MPW6 run). Based on the test results [2, 3, 4] and radiation qualification [5] of these prototypes, the SCA controller underwent a Production Readiness Review on 30 September 2002 [6].

Having passed the Production Readiness Review, the SCA controller, along with three other circuits, were submitted as a multi-project engineering run on 2 February 2003. Two wafers were processes and made available 1 April 2003. Around this time the manufacture discovered a problem in the processing and made two new wafers available on 11 April 2003. These wafers were diced and the SCA controller packaged by Edgetek. 375 packaged SCA controllers arrived in Alberta for testing 3 July 2003. All parts were in good physical condition with no bent pins.

2 Bench Tests

Here we summarise the results of the functional and electrical tests, as well as measurements of how the clock frequency and temperature affects the operation of the SCAC. Full details of the tests can be found in reference [7].

2.1 Functional Tests and Electrical Tests

The functional tests were the same as those used to test the prototype SCAC [2, 3]. 14 parts drew no current and 6 parts failed at least one of the functional tests. A detailed description of the part of the circuit that failed can be found in reference [7]. From the wafer maps supplied by IBM, we anticipated that a total of 362 parts would be totally processed with all layers and vias. This meant that Edgetek had inadvertently packaged 13 parts that would be totally dead and draw no current. We believe that these 13 parts have been identified and that there is one additional part that draws no current for an unknown reason. Since 20 of the 375 parts showed at least one functional or electrical failure, the total yield is 95%. Removing the 13 parts that are known to draw no current, we are left with 7 damaged parts for a functional and electrical yield of 98%.

2.2 Current and Frequency Measurements

We measured the power-supply current drawn by each part while being clocked at 40 MHz. For the 355 working parts, the currents ranged from 108.7 mA to 116.9 mA. The average current was 112.1 mA and the RMS deviation of the currents amongst the parts was 1.5 mA.

Figure 1 shows a histogram of the maximum clock frequency at which each part would run without error. The maximum frequencies ranged from 60.1 MHz to 65.8 MHz. The average maximum frequency was 62.3 MHz and the RMS deviation of the maximum frequencies amongst the parts was 1.1 MHz.

For 13 parts, we measured the current drawn for different clock frequencies. All 13 parts showed a very linear increase in current with clock frequency. The average slope was 0.921 mA/MHz, with an RMS deviation of the slopes amongst the parts of 0.006 mA/MHz. The current at zero clock frequency was between about 73 mA and 82 mA depending on the part.

2.3 Temperature Tests and Burn-in

For 11 parts, we measured the current drawn at a clock frequency of 40 MHz for different temperatures between $-10°$C and 90°C. All 11 parts showed a linear decrease in current with temperature. The average slope was -0.071 mA/°C with an RMS deviation of the slopes amongst the parts of 0.003 mA/°C.

For 11 parts, we measured the maximum clock frequency at different temperatures between $-10°$C and 90°C. The average slope was -0.117 MHz/°C with an RMS deviation of the slopes amongst the parts of 0.003 MHz/°C.

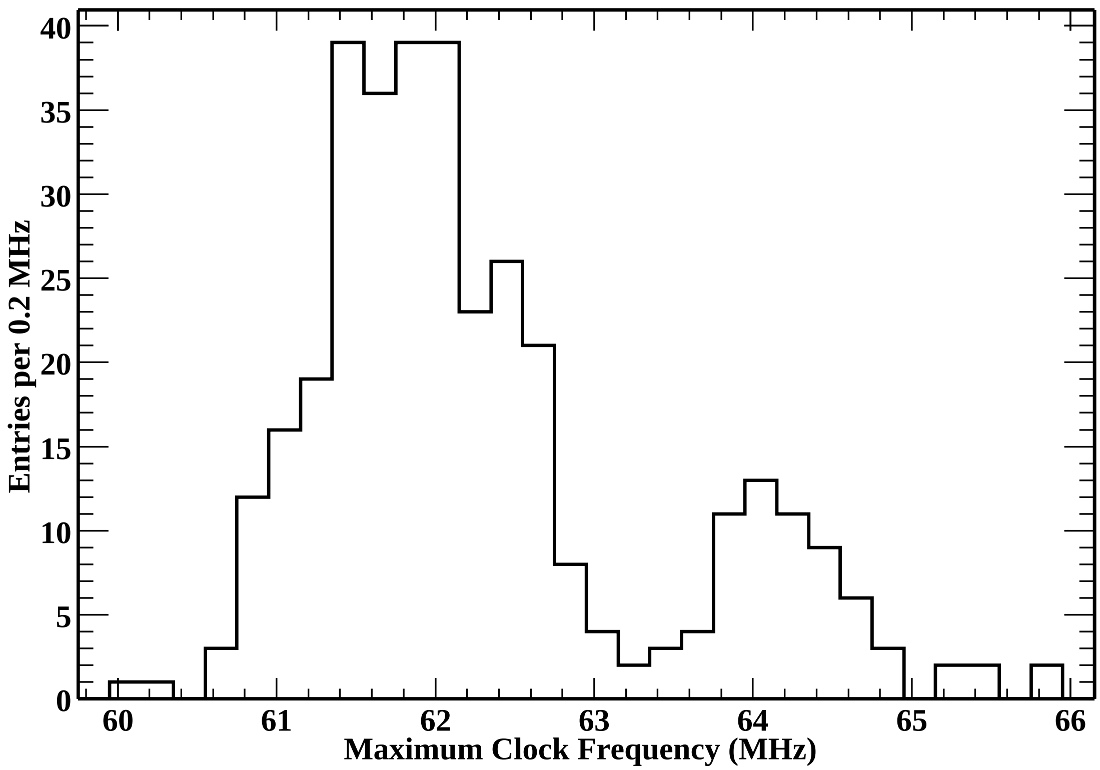

Figure 1: Histogram of the maximum clock frequency of the switched capacitor array controller parts from the engineering run.

As of 4 September 2003, 86 parts have been burnt in at room temperature. The burn-in times ranged from 15.2 hr to 120.6 hr. No failures have been observed during the burn-in tests.

3 Radiation Tolerance Requirements

The SCA controllers are located in the upper region of the front-end board. Although the die of an SCA controller is only 16 mm^2, for safety we consider the radiation levels in a 200 cm^2 area bounded by 300 cm $< Z <$ 320 cm and 330 cm $< R <$ 340 cm. The worst-case simulated radiation levels (SRL) in this region are listed in table 1 for 10 years of LHC operation for the cases of total ionising dose (TID), non-ionising energy loss (NIEL), and single event effects (SEE). The corresponding radiation levels for the endcap crates are approximately ten times smaller than in the barrel.

The ATLAS Policy for Radiation Tolerant Electronics [8] assigns safety factors (SF) which are to be applied in the radiation qualification process. The safety factors account for the uncertainties in the simulated radiation levels (SIM), in possible low dose-rate effects (LDR), and for possible lot-to-lot variations (LOT). Table 1 includes the safety factors we have used. In choosing these safety factors, we have considered the SCA controller to be a radiation-hard ASIC designed in a radiation-qualified deep-submicron CMOS process using

Radiation Effect	SRL (10 yr)	SF			RTC (10 yr)
		SIM	LDR	LOT	
TID	39.7 Gy	3.5	1.5	1	208 Gy
NIEL	1.36×10^{12} n/cm^2	5	1	1	6.81×10^{12} n/cm^2
SEE	3.00×10^{11} h/cm^2	5	1	1	1.50×10^{12} h/cm^2

Table 1: Simulated radiation levels (SRL), safety factors (SF), and radiation tolerance criterion (RTC) applicable to the qualification for production of the SCA controller.

a radiation-tolerant layout technique. The final production of the SCA controller would involve the delivery of a homogeneous batch of 48 wafers. We therefore use values for LOT appropriate to the production of radiation-hard ASICs to be produced in series from a known batch. For the TID tests, we take the LDR safety factor of 1.5 since we do not perform post-irradiation aging at elevated temperatures. The final radiation tolerance criteria (RTC) are calculated as the simulated radiation levels multiplied by the product of the three safety factors:

- $\mathrm{RTC_{TID}} = 208$ Gy,
- $\mathrm{RTC_{NIEL}} = 6.81 \times 10^{12}$ neutron/cm^2 (1-MeV equivalent damage in Si), and
- $\mathrm{RTC_{SEE}} = 1.50 \times 10^{12}$ hadron/cm^2 (hadrons with energy greater than 20 MeV).

4 Previous Radiation Test Results

Details of previous radiation tests with MPW prototypes can be found in reference [5]. A summary of the results is given here.

We have previously irradiated a total of 40 parts with either protons, neutrons, or x-rays. Four of these irradiated parts were from the MPW4 run [9], while the remaining 36 were from the MPW6 run [5].

4.1 Previous TID Test Results

The effects of TID on power supply current have been measured for 26 parts from the MPW6 run and 4 parts from the MPW4 run using x-rays or protons. In no case was there a functional interrupt or upset during the x-ray irradiations. No post-irradiation effects due to high temperature or room temperature annealing were observed. Two parts were pre-stressed by elevated temperature burn-in before irradiation. Again, no effect was observed. The maximum drop in current with proton radiation was 1 mA, or 0.7%, from a dose of 3.2 kGy(SiO_2) or over 7 times the $\mathrm{RTC_{TID}}$ for selection, while the maximum drop in current with x-rays was 4.2 mA, or 3.4%, from a dose of 44 kGy(SiO_2) or over 106 times the $\mathrm{RTC_{TID}}$ for selection.

Further investigations of the change in current after irradiation and with temperature indicate that some of the drop in current (about half) during irradiation can be attributed to thermal heating of the device [10]. We attribute the remaining decrease in current to be due to the nature of the DSM CMOS device: since the gate oxide is thin, the effects of interface traps are dominate and the threshold voltage increases slightly, which causes the sub-threshold current to decrease. This effect is normally masked by the increase in NMOS leakage currents due to the turn-on of parasitic transistors under the isolation and field oxides. Since enclosed transistors and gard rings have been implemented in this design, the parasitic leakage currents have been eliminated. The small decrease in current will be negligible during ATLAS operation.

4.2 Previous NIEL Test Results

Ten parts were irradiated with neutrons [11]. Each part received a fluence of $(1.9 \pm 0.4) \times 10^{13}$ cm^{-2} (1-MeV equivalent in Si). All parts functioned correctly after irradiation. The current drawn by each part was the same before and after irradiation to within the 5% accuracy of the measurements.

We have also used the NIEL of protons in silicon to estimate the equivalent 1-MeV neutron fluence received by each part. Four MPW4 parts and one MPW6 part were irradiated with protons to a higher damage factor than the $\mathrm{RTC_{NIEL}}$ for selection. Ten parts were irradiated with protons to a higher damage factor than $\mathrm{RTC_{NIEL}}$ for production.

There has been no observation of displacement damage in any of the 15 parts. This is not surprising since the SCAC is a pure CMOS device, except for some bipolar diodes used for ESD protection.

4.3 Previous SEE Test Results

Proton SEE testing has been performed on three beam lines at two different facilities (TRIUMF and Harvard). The analysis of the upsets is complicated by the considerable circuit-mitigation techniques that are employed in the SCAC. All single bit upsets (SBU) in the SRAM (SRAM and LFIFO) are corrected in real time and we denote these as “SRAM SBU”. They have no consequence on the operation of the SCAC but are recorded. Multiple-bit upsets (MBIT) in the SRAM and upsets outside of the SRAM (BCID, EVT, SHFT) (D-latch and combinatorial logic) that are not protected by triple-redundant majority-logic we call “single-event functional interrupts” (SEFI). These upsets are real and may effect the operation of the SCAC. Some will be recovered from on the next clock cycle or the next trigger. Others require a reset of the SCAC.

The energy dependence and angle dependence of the upset cross-sections from previous measurements will be presented and compared to the current results in the sections 7.4 and 7.5.

5 Radiation Facilities

To obtain the TID levels we have used an x-ray irradiation facility and a proton irradiation facility. To obtain the NIEL and SEE levels we have used a proton irradiation facility.

5.1 X-Ray Irradiation Facility

We have used an x-ray generator in Alberta for TID studies [12]. The machine operates at a constant electron accelerating potential of 320 kVp and a tube current of 10 mA. The machine is capable of exposure rates up to about 36 R/s. The absorbed dose rate at the die of the device under test (DUT) was estimated to be (46 ± 3) cGy(SiO_2)/s [13].

5.2 Proton Irradiation Facility

The Northeast Proton Therapy Center of the Massachusetts General Hospital (MGH) was used to irradiate parts. We used a single beam energy of 158.7 MeV. Since the beam from the cyclotron was not degraded and there was a momentum-selecting magnet in the beam line, the absolute error on the energy is on the order of 0.2 MeV and the energy spread is less than 1 MeV.

The DUT was mounted in the beam line using an adjustable tripod stand at a location in which the proton beam flux was between 2.4×10^{10} cm^{-2}s^{-1} and 2.8×10^{10} cm^{-2}s^{-1} during nominal operation. The beam was uniform to within 5% out to a radius of 0.5 cm centered on the die of the device.

The proton intensity was measured with a Faraday cup to less than 5% uncertainty. Each DUT was irradiated for a period of time until it received a proton fluence of 2.5×10^{13} cm^{-2}. This fluence took from 15.0 to 17.5 minutes during nominal accelerator operating conditions.

During one of the runs (part 84) the accelerator turned off due to a software-initiated trip. The following day the software was reloaded and the run was continued to obtain the last 25% of the required fluence. During this run it was not possible to calculate a meaningful live time or determine the change in current with dose (due to annealing and thermal effects) for part 84.

6 Radiation Test Setup

The radiation test setup was similar to that described in references [2] and [5]. The power-supply current was read out using a GPIB interface. The monitor counts from the beam line were recorded in real time, thus allowing us to record the proton flux versus time for each run. The proton flux information allowed us to accurately correlate the beam on and off times with our monitoring DAQ. From this information and counters in the FPGA, it was possible to precisely determine the live time of the DUT in the beam for each run. For the five non-interrupted runs, the average live time was 98.7% with an RMS dispersion of the live times amongst the five runs of 0.3%. We have not applied a small live time correction ($\sim 1\%$) since our error is dominated by the uncertainty in the proton fluence.

7 Radiation Test Results

Each part was functionally tested before and after irradiation using the procedure described in references [2] and [3]. The real-time monitoring of the SCA controller included both the measurement of its current and complete functional monitoring of its operation. We irradiated 6 parts with protons and 10 parts with x-rays. The results presented here use parts from the engineering run, but we also refer to radiation test results from the two MPW run [5, 9]. Using a proton beam allows us to simultaneously accumulate TID, NIEL that can be converted to 1-MeV equivalent neutron fluence, and hadrons with sufficient energy to cause SEE. No occurrences of latch-up were observed and it was not necessary during any of the tests to cycle the power to the SCA controller.

7.1 TID Test Results

The current drawn by each part was monitored during both the x-ray and proton irradiations. As the integrated dose increased, the current exhibited the usual slight decrease [5, 10]. Plots of the change in current versus absorbed dose for each part during x-ray and proton irradiations are shown in figure 2. The total absorbed dose was (2.5 ± 0.2) kGy(SiO_2) for the x-ray exposures and (18 ± 1) kGy(SiO_2) for the proton exposures. Table 2 summarises the results of the TID testing. The current dropped on average by 1.4 mA, or 1.3%, after the device absorbed 2.5 kGy(SiO_2) from x-rays, and dropped on average by 2.0 mA, or 1.8%, after the device absorbed 18 kGy(SiO_2) from protons with energy of 159 MeV. About 18% of the current drop in the case of x-rays was due to thermal heating of the device. In no case wa

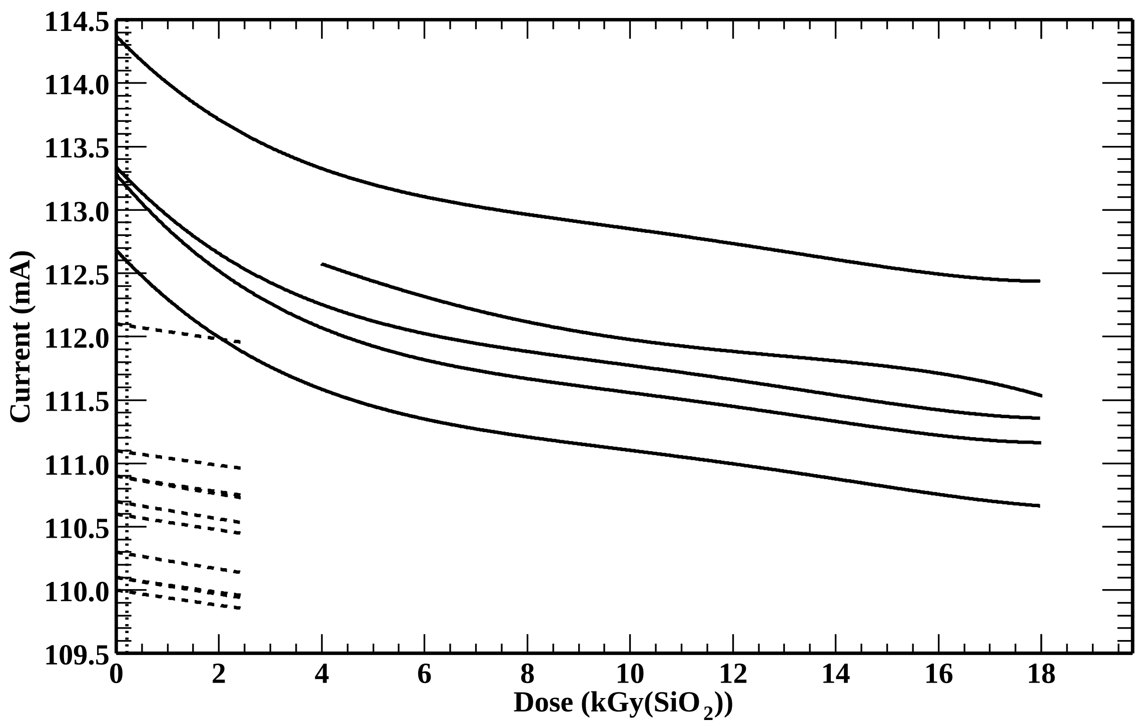

Figure 2: Current versus absorbed dose during x-ray irradiations for ten different parts (dashed lines) and during proton irradiations with energy of 159 MeV for five different parts (solid lines). The doted vertical line at 0.2 kGy(SiO_2) is the radiation tolerance criteria.

X-Ray Irradiation		
Part	Current (mA)	Change (%)
1	−1.4	−1.2
33	−1.4	−1.3
36	−1.4	−1.3
64	−1.4	−1.3
115	−1.5	−1.3
171	−1.5	−1.3
200	−1.4	−1.3
245	−1.4	−1.3
306	−1.4	−1.3
Proton Irradiation		
Part	Current (mA)	Change (%)
52	−2.1	−1.9
179	−2.0	−1.8
285	−2.1	−1.9
292	−2.0	−1.7

Table 2: Changed in current for the parts after absorbing either a total ionizing dose of 2.5 kGy(SiO_2) from x-rays or 18 kGy(SiO_2) from protons with energy of 159 MeV.

7.2 NIEL Test Results

For protons with energy of 159 MeV, the NIEL in silicon is about 2.64 keV cm^2g^{-1} and the relative displacement damage (K_p/K_n) is 1.3. For a proton fluence of $2.5 \times 10^{13}cm^{-2}$, the NIEL of protons in silicon is equal to the equivalent 1-MeV neutron fluence of $3.2 \times 10^{13}cm^{-2}$. Six parts have been irradiated beyond the RTC_{NIEL} level.

7.3 SEE Test Results

Six parts were irradiated with protons of energy 159 MeV to a fluence of 2.5×10^{13} cm^{-2}. The proton beam impinged on the DUT at a different angle for each part. Table 3 summaries the upset results for the proton SEE tests. The meaning of the different types of upsets is explained in section 4.3 and reference [5].

7.4 Angular Dependence of the Upsets

The particle fluxes at the location of the SCA controllers are expected to be homogeneous in direction. Most SEE testing is performed with the beam impinging on the device at right angles to the largest surface of the die ($\theta = 0°$). There is some evidence that for devices that

Part	Angle (degree)	Upsets					
		SRAM	LFIFO	BCID	EVT	SHFT	MBIT
292	0	296	113	2	1	12	3
52	20	307	130	2	1	20	7
179	45	339	140	3	0	33	10
285	70	386	159	4	5	35	6
84	90	378	147	3	2	33	7
259	180	432	162	3	2	14	6

Table 3: Proton beam angle and observed upsets for each part.

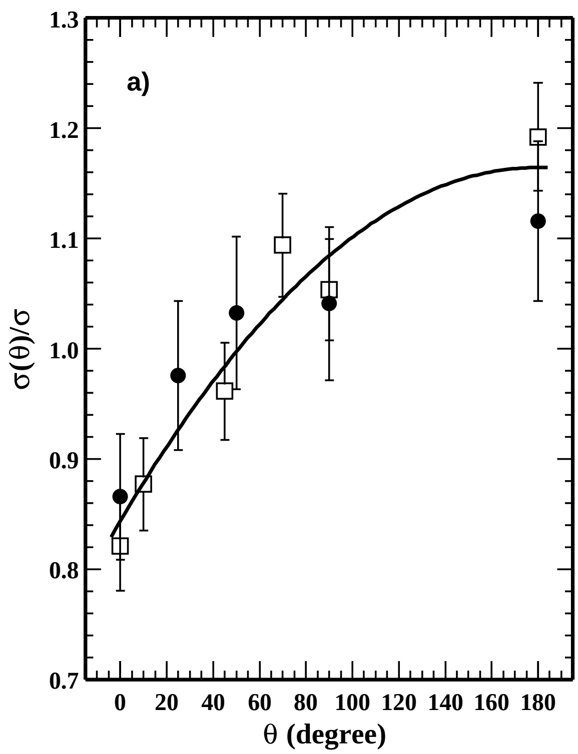

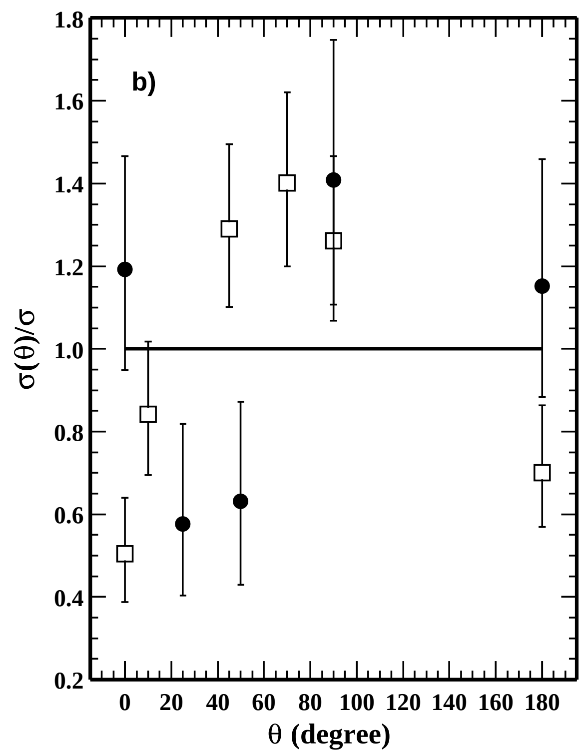

Figure 3: Ratio of the proton-induced upset cross-section at angle θ to the cross-section averaged over all angles: a) SRAM SBU and b) SEFI that could not be corrected by the SCA controller logic. The solid circles are for engineering prototype parts with a proton beam energy of 159 MeV, while the open squares are for MPW6 prototype parts with a proton beam energy of 491 MeV.

have a high critical charge and one small dimension, that there is an angular dependence in the proton-induced SEU cross-section [14].

We irradiated devices at six different angles with protons of energy 159 MeV. A high energy was chosen so that the effects of the materials in the packaging and the printed circuit board could be neglected. The upset cross-section relative to the average upset cross-section for all angles is shown in figure 3. In making this plot we have assumed the uncertainty in the proton fluence cancels. Figure 3a) shows the cross-sections for SRAM SBU, while figure 3b) shows the cross-section for SEFI in the registers and the multiple-bit upsets in the SRAM. Shown for comparison, as the open squares, are previous data taken with MPW6 parts at a proton energy of 491 MeV [5, 15]. Both distributions are consistent with no angular dependence, although a small increase in the SRAM SBU cross-section with increasing angle may be possible.

7.5 Impact of SEE on ATLAS Operation

The upsets can be divided into two classes. The single-bit SRAM upsets which are corrected on-the-fly (SRAM and LFIFO upsets) and the non-correctable upsets (MBIT, BCID, EVT, SHFT upsets). Figure 4 shows the total upset cross-section and cross-section for the upsets that could not be corrected by the SCA controller logic. The total upset cross-section is dominated by the single-bit upsets occurring in the SRAM. Included in the plot is data take at four different proton beam lines using parts from three different fabrication runs. Table 4 summarises the different data used in figure 4.

Data Marker in Figure 4	Fabrication Run	Proton Facility
solid triangle	engineering	MGH
solid circle	MPW6	TRIUMF 2C
solid square	MPW6	TRIUMF 1B
open circle	MPW4	Harvard

Table 4: Explanation of the different data sets used in figure 4.

We found it difficult to fit the upset cross-sections versus energy to either the standard Weibull or log-normal cumulative distribution functions when using all the data. There appears to be a possible normalization difference between the data set from the Harvard cyclotron (MPW4) and the three other data sets. We have thus excluded the MPW4 data set from the fits. The remaining data has been fit to a log-normal cumulative density function and the results of the fits are shown in table 5. These fits give directly the cross-section at infinite energy (saturation cross-section), σ_{sat}, and the energy at which the saturation cross-section drops by 50% (threshold energy), E_{th}. W is a shape parameter.

We have convoluted the fitted upset distributions in figure 4 with the simulated energy spectra for protons, pions, and neutrons [5]. This calculation results in the upset rates in ATLAS shown in the second column of table 6 and the mean time between upsets (MTBU) shown in the third column. These upset rates can be scaled to the entire EM barrel system by taking into account the fact that a total of 1792 SCA controllers are required to instrument

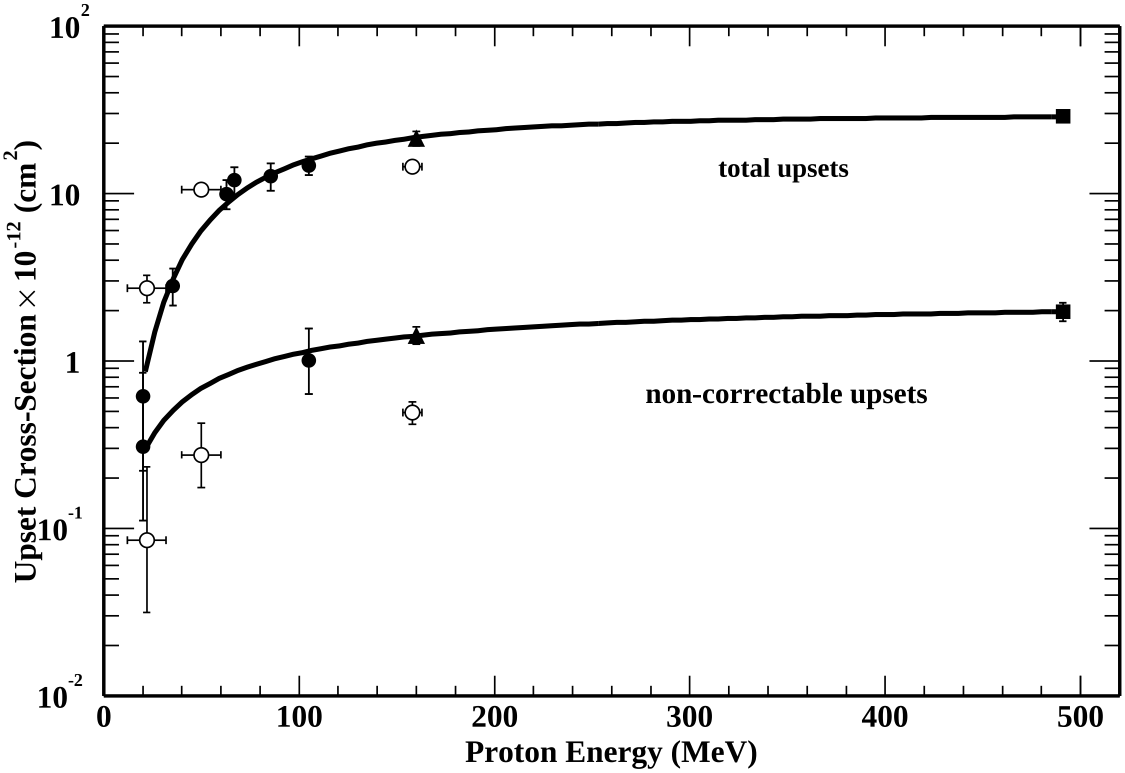

Figure 4: Proton-induced upset cross-sections for the SCA controller: total upsets (upper data) and SEFI that could not be corrected by the SCA controller logic (lower data). The solid circles are data taken with 2C beam line at TRIUMF, the solid squares are data taken with the 1B beam line at TRIUMF, the solid triangles are data taken with the Northeast Proton Therapy Center at the Massachusetts General Hospital, and the open circles are data taken at Harvard Cyclotron Laboratory. The open-circle data is not included in the fit.

Parameter	Total Upsets	Non-Correctable Upsets
σ_{sat} (10^{-12} cm^2)	29^{+3}_{-3}	2.3 ± 1.4
E_{th} (MeV)	96^{+20}_{-13}	105 ± 124
W (MeV)	$2.2^{+0.4}_{-0.3}$	4 ± 7
χ^2/dof	0.2	0.05

Table 5: Result of fits to the upset cross-section data using a log-normal cumulative density function.

the EM barrel (896 front-end boards, with 2 SCA controllers per board). Scaling by 1792 gives the fourth column of data in table 6. The upper half of table 6 includes all the upsets, most of which are correctable, while the lower half of the table 6 shows the corresponding rates for upsets that are not correctable by the SCA controller.

Total Upsets			
Particle Type	Upset Rate (10^{-11} s^{-1}/device)	MTBU (10^3 device-day)	(ATLAS-day)
proton	5.6	208	116
pion	8.2	141	79
neutron	322	3.6	2.0
hadron	336	3.4	1.9
Non-Correctable Upsets			
Particle Type	Upset Rate (10^{-12} s^{-1}/device)	MTBU (10^4 device-day)	(ATLAS-day)
proton	4.5	256	1430
pion	5.8	199	1110
neutron	275	4.2	23
hadron	285	4.1	23

Table 6: Prediction of upset rates and mean time between upsets (MTBU) in the SCA controller for different particle types in ATLAS.

8 Summary of Radiation Test Results

Sixteen parts have been irradiated well beyond the radiation tolerance criteria for TID. We might expect a current drop of about 20 μA, or 0.02%, during the 10 years of operation in ATLAS. Since no upsets or significant parameter variations have been observed, we consider the SCA controller qualified for TID radiation.

There has been no observation of displacement damage in any of the parts. Six parts have been irradiated to greater than four times the radiation tolerance criteria for NIEL by using protons. In any case, it is not necessary to test for NIEL damage for pure CMOS devices, which are naturally tolerant to displacement damage [8]. Although the SCA controller uses bipolar diodes for the ESD protection, these diodes have been shown to be immune to displacement damage.

Six parts have been irradiated with protons with energy of 159 MeV and the soft upset cross-sections measured. In no case was a hard upset observed. The soft upset rates are considered not to impose a significant problem with the operation of ATLAS. We consider the SCA controller qualified for SEE.

Based on the radiation test results presented here and previously in reference [5], we consider the SCA controller radiation qualified for production.

References

[1] S. Böttcher, J. Parsons, W. Sippach, D. Gingrich, "Deep Submicron Implementation of the ATLAS LAr SCA Controller",
http://www.nevis.columbia.edu/~atlas/electronics/asics/scac/scac-dsm.ps

[2] S. Liu, D.M. Gingrich, W. Syed, "Tests of the First Prototype SCA Controller",
http://csr.phys.ualberta.ca/gingrich/atlas/notes/scac-mpw4.pdf

[3] S. Liu, D.M. Gingrich, W. Syed, "Tests of the Final Prototype SCA Controller",
http://csr.phys.ualberta.ca/gingrich/atlas/notes/scac-mpw6.pdf

[4] D.M. Gingrich, S. Liu, "Stress Tests",
http://csr.phys.ualberta.ca/gingrich/atlas/notes/scac-stress.pdf

[5] D.M. Gingrich, N.J. Buchanan, S. Liu, W. Syed, "Radiation Qualification of the SCA Controller Preselection", ATL-LARG-2003-002,
http://csr.phys.ualberta.ca/gingrich/atlas/notes/larg-2003-002.pdf

[6] "Production Readiness Review of the Larg DSM ASICs. Report", ATC-RA-ER-0029,
http://agenda.cern.ch/fullAgenda.php?ida=a021106

[7] D. Gish, B. Gilday, D.M. Gingrich, S. Liu, "Tests of the Engineering Run SCA Controller"
http://csr.phys.ualberta.ca/gingrich/atlas/notes/scac-engineering.pdf

[8] M. Dentan, P. Farthouat, M. Price, "Atlas policy on radiation tolerant electronics", ATC-TE-QA-0001 (2000);
http://atlas.web.cern.ch/Atlas/GROUPS/FRONTEND/radhard.htm
We have used values from the updated simulations of January 2003.

[9] S. Böttcher, S. Negroni, J.A. Parson, S. Simon, "Status of Functional and Radiation Testing of the Deep Submicron SCA Controller",
http://www.nevis.columbia.edu/~atlas/electronics/asics/scac/SCACtest.ps

[10] D.M. Gingrich, "Thermal Effects in the SCAC",
http://csr.phys.ualberta.ca/gingrich/atlas/notes/scac-thermal.pdf

[11] D.M. Gingrich, "Neutron Test",
http://csr.phys.ualberta.ca/gingrich/atlas/notes/scac-neutron.pdf

[12] D.M. Gingrich, N.J. Buchanan, C. Cojocaru, W. Syed, "X-Ray Facility in the Centre for Subatomic Research at the University of Alberta",
http://csr.phys.ualberta.ca/gingrich/atlas/notes/xray-machine.pdf

[13] D. Gish, "X-Ray Dosimetry of the Switched-Capacitor Array Controller",
http://csr.phys.ualberta.ca/gingrich/atlas/notes/xray-dose.pdf

[14] R.A. Reed *et al*, "Evidence for Angular Effects in Proton-Induced Single-Event Upsets", IEEE Trans. Nucl. Sci., vol. 49, pp. 3038-3044, Dec. 2002.

[15] D.M. Gingrich, N.J. Buchanan, "Angular Effects", `http://csr.phys.ualberta.ca/gingrich/atlas/notes/scac-angle.pdf`